

Cell Reports, Volume 42

Supplemental information

**Vaginal epithelial dysfunction is mediated
by the microbiome, metabolome, and mTOR signaling**

Alicia R. Berard, Douglas K. Brubaker, Kenzie Birse, Alana Lamont, Romel D. Mackelprang, Laura Noël-Romas, Michelle Perner, Xuanlin Hou, Elizabeth Irungu, Nelly Mugo, Samantha Knodel, Timothy R. Muwonge, Elly Katabira, Sean M. Hughes, Claire Levy, Fernanda L. Calienes, Douglas A. Lauffenburger, Jared M. Baeten, Connie Celum, Florian Hladik, Jairam Lingappa, and Adam D. Burgener

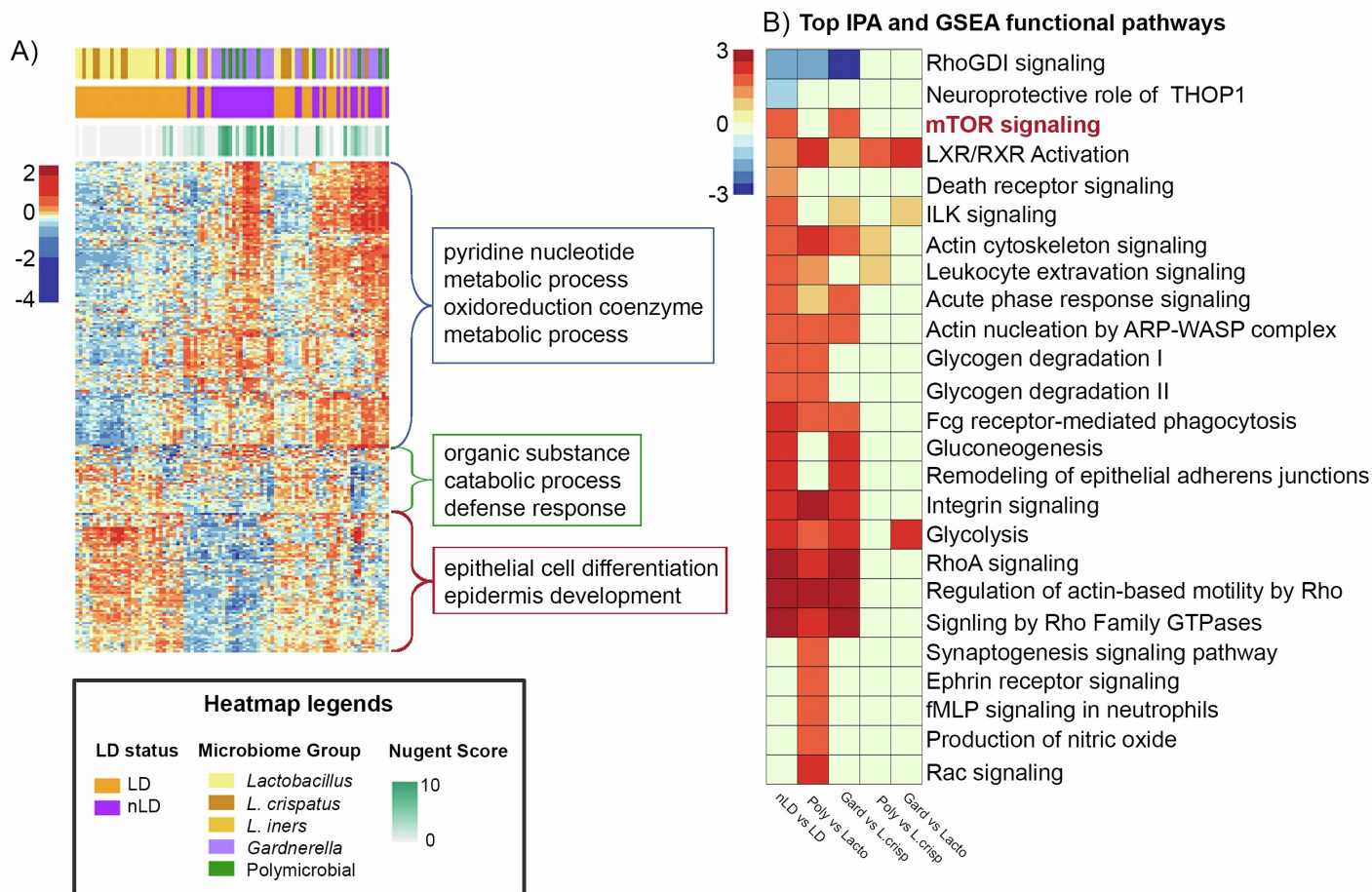
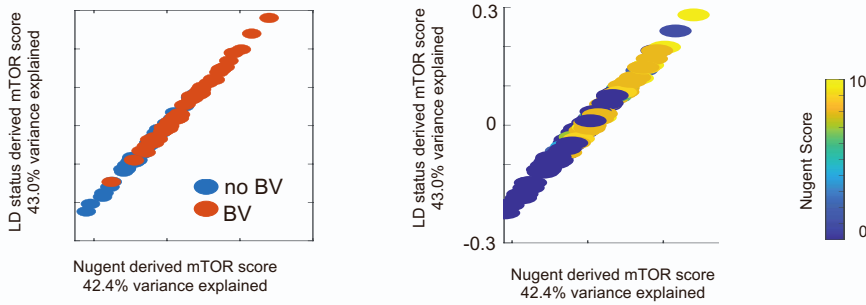
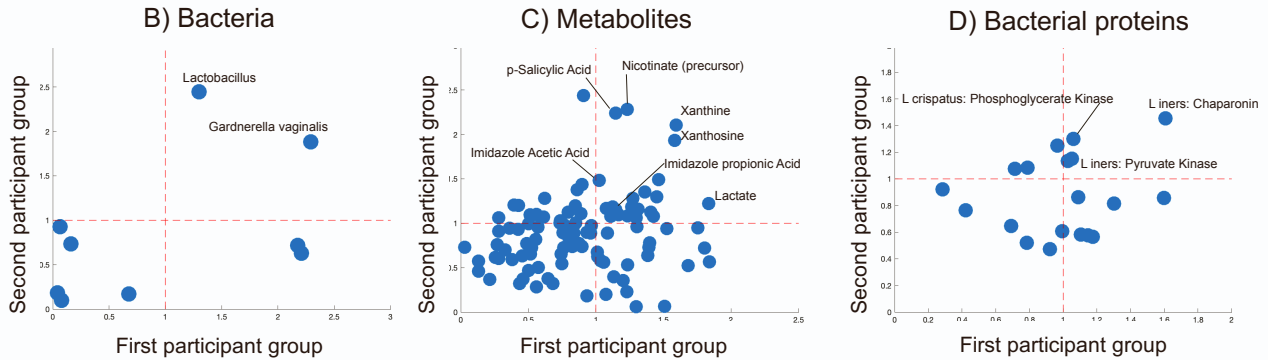


Figure S1. Participant group 2 proteomics, Related to Figure 2: Validation of the molecular changes and functional proteome differences between microbiome groups in vaginal mucosal fluid samples. a) 246 of 454 proteins in the mucosal fluid taken from the second participant group were significantly different (5% FDR) between LD (orange) and nLD (purple) groups. Hierarchical clustering of these proteins showed similar differences between microbiome groups as the larger participant group (Figure 2a), including small molecule metabolic processes ($p < 0.005$), cell differentiation ($p = 1.7E-5$), epithelial adherens remodeling ($p = 3.6E-6$), integrin ($p = 1E-4$) and Rho signaling ($p = 6E-7$). b) Canonical pathways differences between microbiome groups were also the same as the first participant group (Figure 2c), with gene set enrichment analysis (GSEA) identifying mTOR signaling differences as the top (and only) pathway significant between microbiome groups, whereas ingenuity pathway analysis (IPA) identifying more pathways (others listed in figure).

A) mTOR score derivation comparison: Spearman Rho = 0.995



B-D) Comparing participant groups: Mucosal fluid mTOR score predictors



E-G) Second participant group: Predictors of mTOR scores between sample types

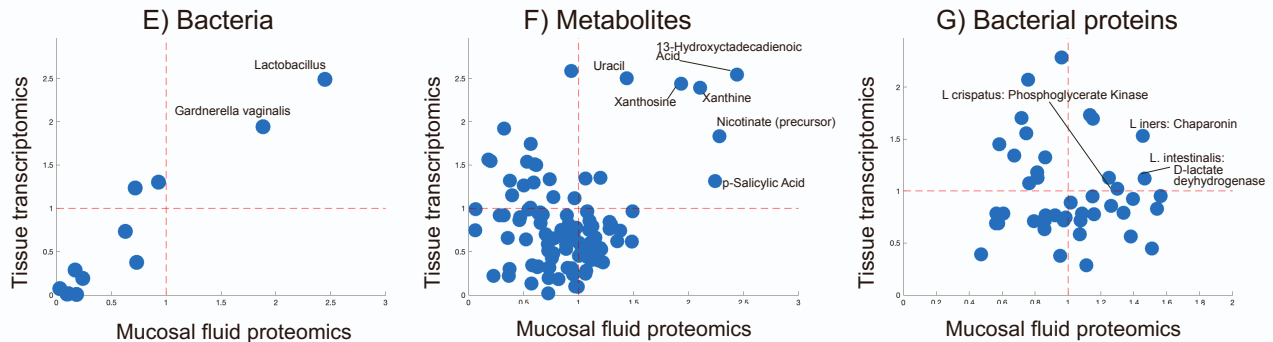
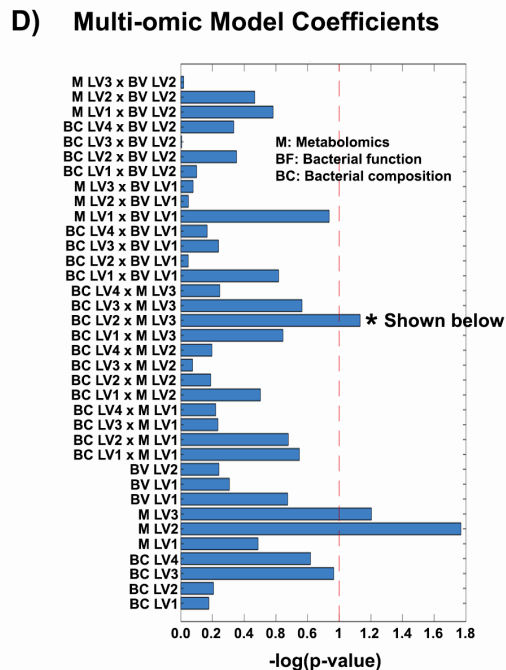
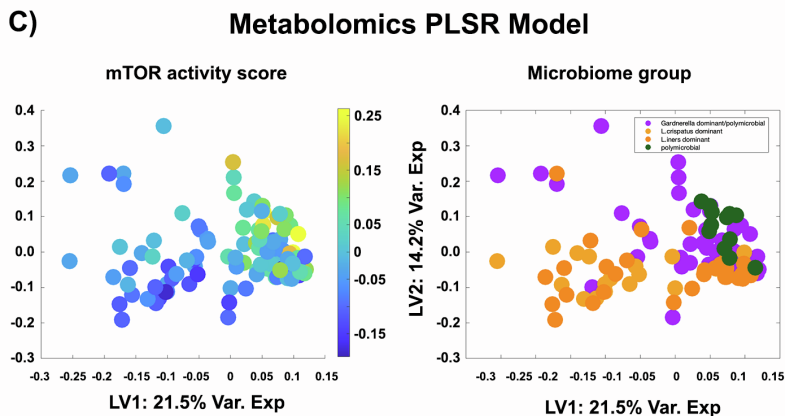
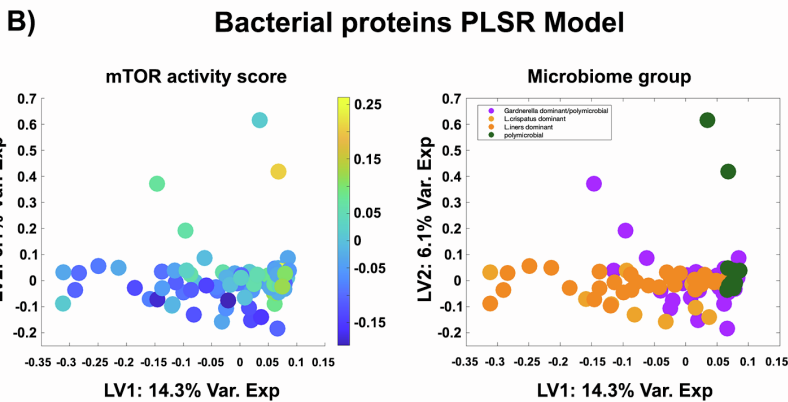
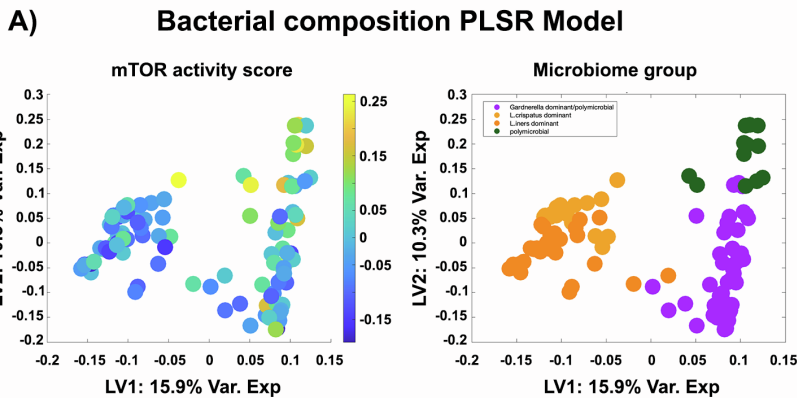


Figure S2. Vaginal mTOR activity correlated with either LD status and Nugent score in women can be predicted from the microbiome and metabolites present in the vaginal environment, Related to Figure 3 and Figure 4. A continuous approach (i.e. Spearman correlation, PLS-R) regressing the mTOR proteins against Nugent score could also be used to generate the mTOR score variable for downstream modeling rather than the binary approach that was used in Figure 4. To assess this, we re-calculated the mTOR score using a continuous PLS-R of mTOR pathway proteins against the Nugent score. We found that the correlation between the mTOR score derived by the Nugent Score and LD-Status approaches were nearly identical (Spearman rho = 0.995), that the Nugent Score derived mTOR score showed higher mTOR score was associated with higher BV Nugent Score, and the latent variables derived from the mTOR proteins by each approach explained comparable variation in LD-Status and Nugent Score. Comparison of (B) Bacterial composition (C) metabolites and (D) bacterial proteins predictive of proteomics-derived mTOR score in both groups of women. Top bacteria that predicted mTOR activation included *Gardnerella* and *Lactobacillus* species. Metabolites predicting mTOR include xanthine, xanthosine, and imidazole propionic acid. The coverage of the mTOR signaling pathway was greater when analyzing the transcriptomics of the vaginal tissues. Comparison of (E) Bacterial composition (F) metabolites and (G) bacterial proteins that predicted activated mTOR signaling in the smaller validation participant group where mTOR activity was inferred via transcriptomics (X-axis) or proteomics (Y-axis). Top bacteria that predicted mTOR activation included *Lactobacillus* and *Gardnerella*. Mucosal metabolites predicting mTOR activity include 13-hydroxyctadecadienoic acid, nicotinate, p-Salicylic acid, and uracil.



E) Bacterial composition LV2 and Metabolome LV3

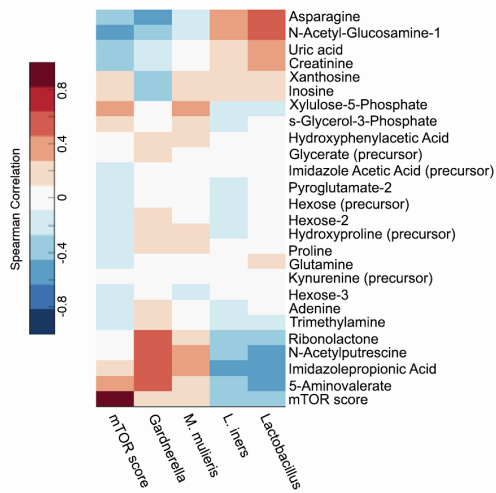
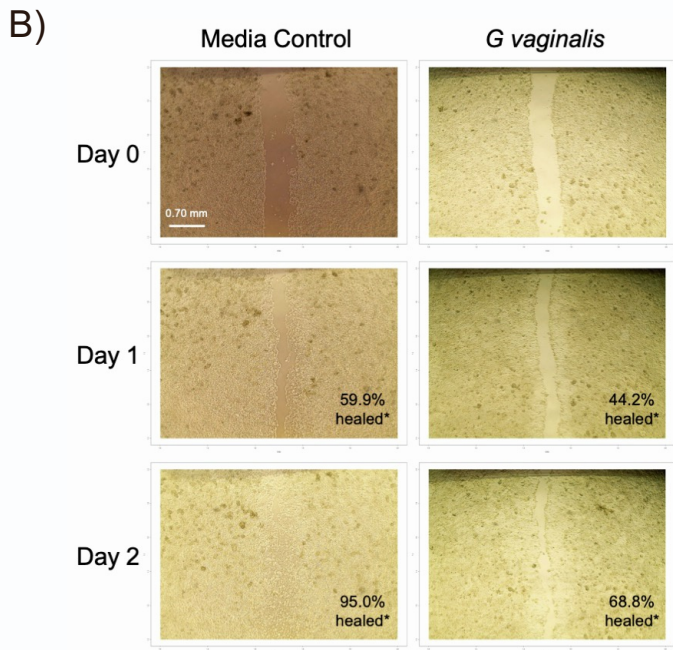
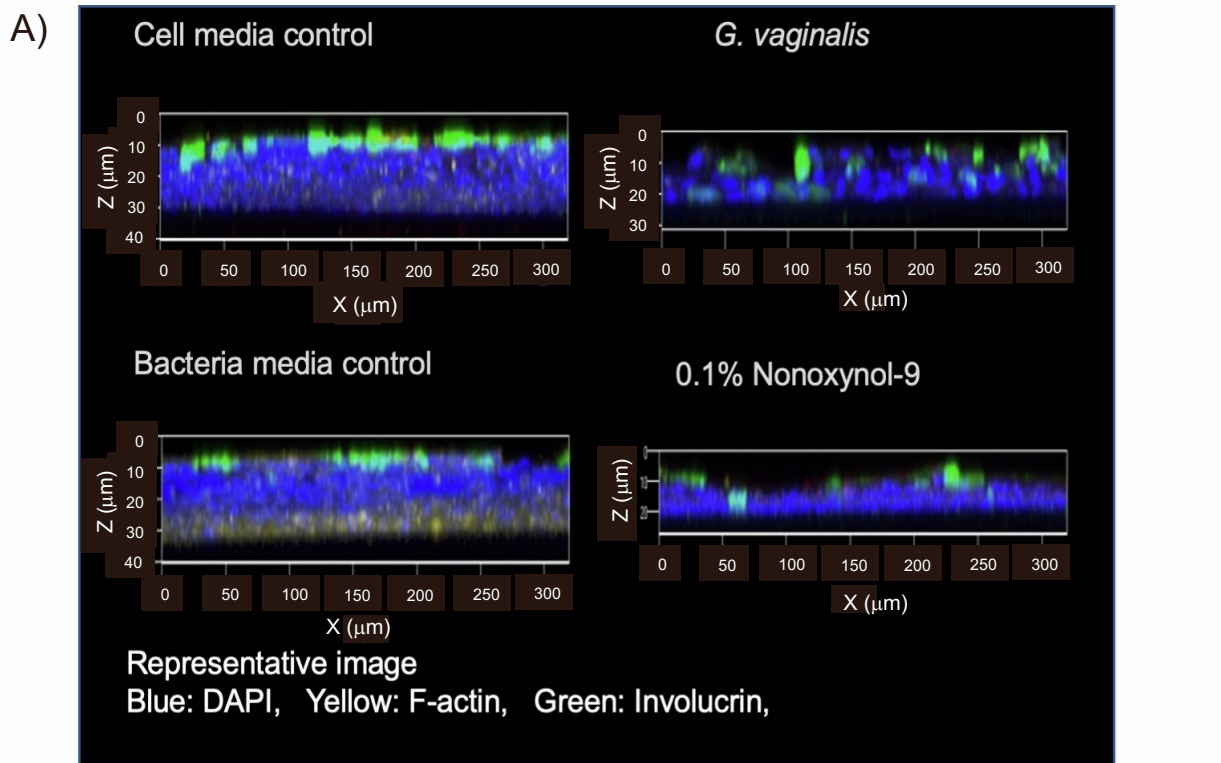


Figure S3: Host mTOR activity calculated using Pathway Interaction Database protein expressions shows same associations with bacterial variables and host immune, barrier functions as the GSEA protein list, Related to Figure 4. The mTOR activity score (method described in Figure 3) that was calculated using mucosal fluid protein expression of mTOR proteins identified using the PID database was regressed against (A) bacterial taxa, (B) bacterial proteins and (C) metabolites measured in the vaginal fluid. The top significant factors correlated with the PID mTOR score also correlated with the GSEA mTOR score, indicating a robustness of the data.



*% healed compared to D0 measurement of same scratch

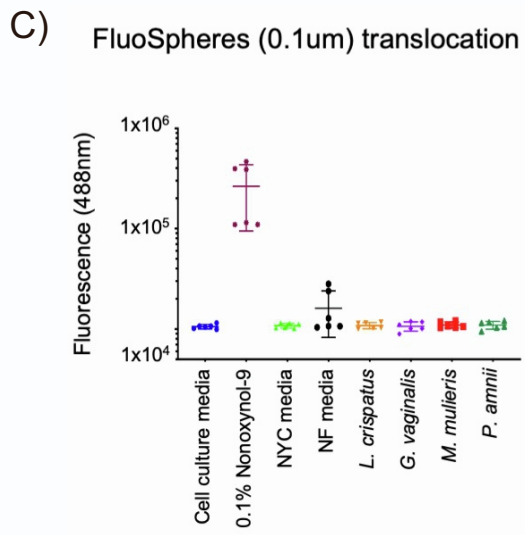


Figure S4: Physiological assays to test vaginal barrier integrity in the presence of bacterial products from four common vaginal bacterial species, Related to Figure 5. (A) A representative image of *G. vaginalis*, as well as the positive control, causing a significant decrease in thickness of VK2 multicellular growth. Measurements of this assay are summarized in Figure 6c. (B) A representative image of *G. vaginalis*, as well as a negative control, where *G. vaginalis* inhibited wound healing which was evident by Day 2 post-scratch (40x magnification). (C) 0.1% Nonoxynol-9 induced a leaky-barrier large enough for virus sized particles to translocate across the barrier, however none of the bacterial supernatant conditions caused this same effect. Error bars represent standard deviation of the mean; n=6.

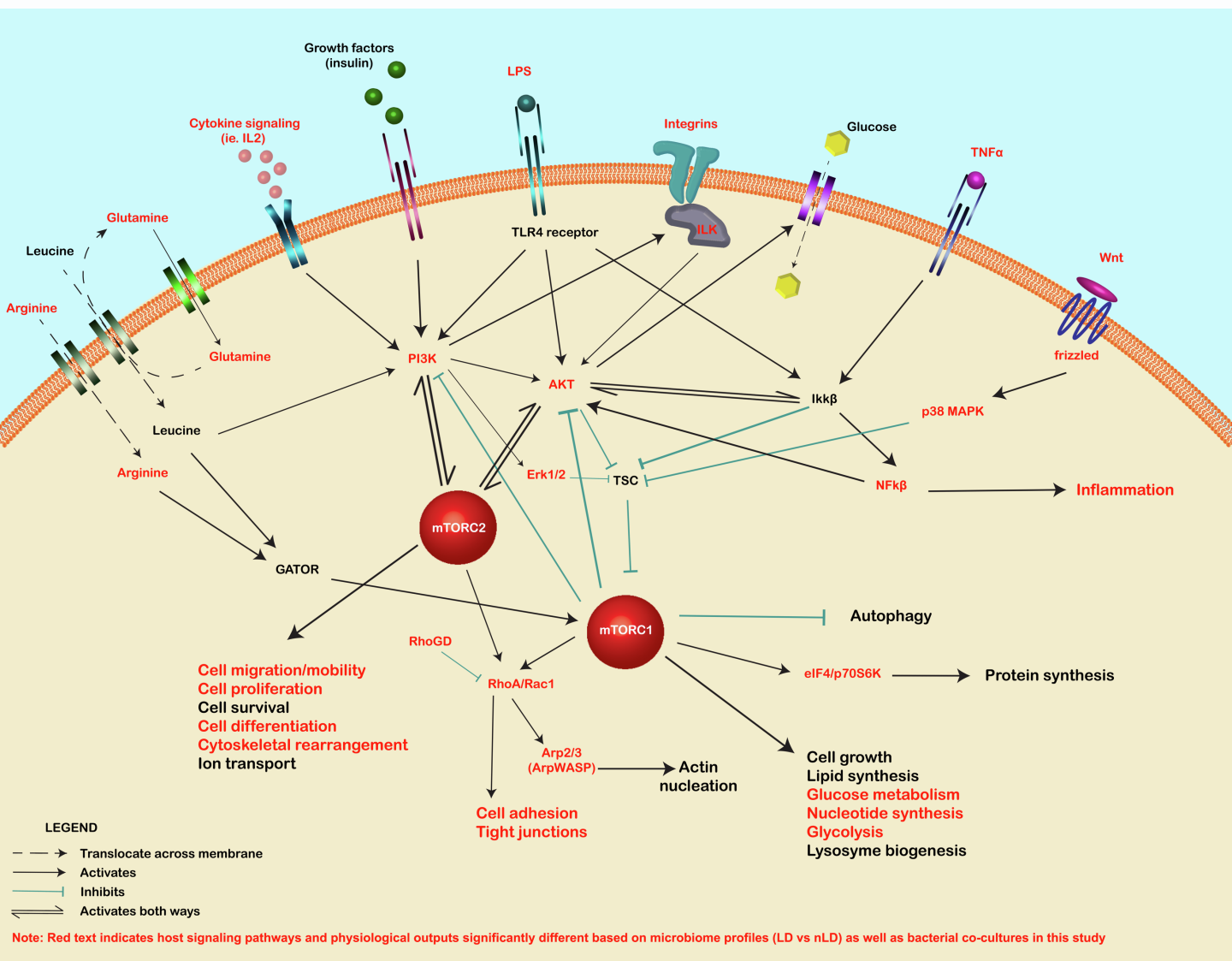


Figure S5: mTOR signaling pathways modulated by the vaginal microbiome, Related to Figure 2. Summarization of host intracellular signaling pathways associated with the microbiome. **Red** indicates signaling pathways, factors and outputs that were differentially expressed between non-*Lactobacillus* and *Lactobacillus* dominant microbiome groups.